Comparison of MRI artificial intelligence-guided cognitive fusion-targeted biopsy versus routine cognitive fusion-targeted prostate biopsy in prostate cancer diagnosis: a randomized controlled trial

Ruiyi Deng[1,2,3†], Yi Liu[1,2,3†], Kexin Wang[4], Mingjian Ruan[1,2,3], Derun Li[1,2,3], Jingyun Wu[6], Jianhui Qiu[1,2,3], Pengsheng Wu[5], Peidong Tian[1,2,3], Chaojian Yu[1,2,3], Jiaheng Shang[1,2,3], Zihou Zhao[1,2,3], Jingcheng Zhou[1,2,3], Lin Cai[1,2,3], Xiaoying Wang[6]* and Kan Gong[1,2,3]*

Abstract

Background Cognitive fusion MRI-guided targeted biopsy (cTB) has been widely used in the diagnosis of prostate cancer (PCa). However, cTB relies heavily on the operator's experience and confidence in MRI readings. Our objective was to compare the cancer detection rates of MRI artificial intelligence-guided cTB (AI-cTB) and routine cTB and explore the added value of using AI for the guidance of cTB.

Methods This was a prospective, single-institution randomized controlled trial (RCT) comparing clinically significant PCa (csPCa) and PCa detection rates between AI-cTB and cTB. A total of 380 eligible patients were randomized to the AI-cTB group ($n = 191$) or the cTB group ($n = 189$). The AI-cTB group underwent AI-cTB plus systematic biopsy (SB) and the cTB group underwent routine cTB plus SB. The primary outcome was the detection rate of csPCa. The reference standard was the pathological results of the combination of TB (AI-cTB/cTB) and SB. Comparisons of detection rates of csPCa and PCa between groups were performed using the chi-square test or Fisher's exact test.

Results The overall csPCa and PCa detection rates of the whole inclusion cohort were 58.8% and 61.3%, respectively. The csPCa detection rates of TB combined with SB in the AI-cTB group were significantly greater than those in the cTB group at both the patient level (58.64% vs. 46.56%, $p = 0.018$) and per-lesion level (61.47% vs. 47.79%, $p = 0.004$). Compared with cTB, the AI-cTB could detect a greater proportion of patients with csPCa at both the per-patient level (69.39% vs. 49.71%, $p < 0.001$) and per-lesion level (68.97% vs. 48.57%, $p < 0.001$). Multivariate logistic analysis indicated that compared with the cTB, the AI-cTB significantly improved the possibility of detecting csPCa ($p < 0.001$).

---

†Ruiyi Deng and Yi Liu contributed equally to this work and should be considered co-first authors.

*Correspondence:
Xiaoying Wang
wangxiaoying@bjmu.edu.cn
Kan Gong
kan.gong@bjmu.edu.cn
Full list of author information is available at the end of the article

Deng *et al. BMC Medicine*   (2024) 22:530

Page 2 of 13

Conclusions AI-cTB effectively improved the csPCa detection rate. This study successfully integrated AI with TB in the routine clinical workflow and provided a research paradigm for prospective AI-integrated clinical studies.

Trial registration ClinicalTrials.gov, NCT06362291.

Keywords Prostate cancer, Artificial intelligence, Cognitive targeted biopsy, Diagnosis, Randomized controlled trial

Background

Prostate cancer (PCa) is one of the most prevalent malignancies in the male population [1]. Prostate biopsy plays a crucial role in the diagnosis, risk stratification, and treatment planning of PCa. Over the past 10 years, significant advancements have occurred in the field of PCa imaging and diagnosis, primarily due to the introduction of innovative techniques and technologies such as multiparametric magnetic resonance imaging (mpMRI) and targeted biopsy [2]. In current medical practice, it is recommended and considered essential to conduct mpMRI of the prostate before conducting a biopsy procedure [1].

There are several strategies for target biopsy, such as cognitive fusion targeted biopsy (cTB), in-bore MRI target biopsy (MRI-TB), and MRI-transrectal ultrasound (TRUS) fusion target biopsy (FUS-TB) [3]. There is still no consensus on which strategy for TB should be preferred [3, 4]. Most of the previous studies demonstrated no overall difference in clinically significant PCa (csPCa) or PCa among the three TB strategies [3]. cTB involves a urologist visually inspecting the ultrasound images in real time and then cognitively targeting the MRI-identified lesion using TRUS guidance [3]. It is simple and convenient to conduct cTB with no additional financial expenses or time investments related to acquiring and implementing such software. Successful implementation of prostate biopsy requires the acquisition of correct image interpretation, proper processing of MR images for biopsy guidance, and precise sampling of targeted suspicious lesions with MRI data [5]. However, visual assessment of MR images based on visual features of lesions, such as size, location, and intensity, requires high-level operator expertise, leading to interoperator variability [6]. There is a steep learning curve for the interpretation of MR images [7]. In addition, some features of MR images reflecting tumor heterogeneities and some lesions with low volumes may be missed in visual assessments. These invisible lesions may be associated with PCa aggressiveness and progression [6]. Furthermore, if investigators are unable to accurately identify patients who are at a greater risk of csPCa and primarily rely on increasing the number of biopsies performed to ensure the detection of csPCa, this will inevitably lead to more unnecessary biopsies, increasing the risk of complications such as infection and bleeding, increasing the pain and burden of patients, and causing a great waste of medical resources [8]. Therefore, it is crucial for PCa patient diagnosis, surveillance, treatment planning, and management to investigate and develop approaches that can accurately detect and identify patients with csPCa and further optimize prostate biopsy procedures.

In recent years, there have been remarkable advancements in the field of artificial intelligence (AI) techniques, particularly in the medical domain. These AI techniques have demonstrated the ability to significantly enhance various medical tasks, such as tumor detection, classification, and prognosis prediction [8]. Increasing evidence supports the ability of AI to facilitate precise diagnosis of PCa and assist in therapeutic decisions [9, 10]. Compared with doctors, AI has the potential to identify not only holistic tumor morphology but also task-specific and granular radiological patterns that cannot be detected by the naked eye [8]. Therefore, AI has great potential to reduce inconsistencies between observers and improve diagnostic accuracy [11]. Although several studies have explored the application of AI in assisting radiologists in interpreting PCa MR images, the incorporation of AI into prostate MR images and TB workflows is still limited [5]. The interactions between doctors and AI are insufficient, and there is a lack of clinical translation of AI. In addition, most of the existing prostate MRI AI studies are retrospective, prospective, and well-designed clinical trials are warranted for further investigating the application of AI in PCa premise diagnosis.

Previous AI studies at our institution have developed deep learning-based AI models trained on MR images that achieve good performance in the detection and localization of csPCa [12]. Furthermore, the trained AI algorithms were embedded into proprietary structured reporting software, and radiologists simulated their real-life work scenarios to interpret and report the PI-RADS category of each patient using this AI-based software. The multicenter validation results showed that AI software substantially improved the lesion-level and patient-level specificity of the readers while preserving patient-level sensitivity in detection and increased the diagnostic confidence for csPCa diagnosis [13]. In this prospective randomized controlled trial (RCT), we compared the cancer detection rates of AI-cTB and routine cTB and explore the added value of using AI for the guidance of targeted biopsy of PCa.

Deng *et al. BMC Medicine*   (2024) 22:530

Page 3 of 13

Methods

Trial design and oversight

This prospective, single-institution RCT compared the csPCa and PCa detection rates of the AI-cTB and routine cTB. The study was reviewed and approved by the institutional review board of our institution (2023IR27). The trial was registered on the ClinicalTrials.gov (NCT06362291). The Consolidated Standards of Reporting Trials (CONSORT) flow diagram of the study is shown in Fig. 1.

Study population and outcomes

Patients were prospectively enrolled at Peking University First Hospital (Beijing, China) from August 2023 to March 2024. All subjects provided written informed consent for prospective data analysis.

The inclusion criteria were (1) age ≥ 45 years and ≤ 85 years; (2) prostate biopsy, including patients with suspicious prostate nodes found by digital rectal examination (DRE), suspicious lesions found by TRUS or MRI, and a verified prostate-specific antigen (PSA) increase to 4–20 ng/ml; and (3) no previous prostate biopsy. The exclusion criteria were (1) contraindication to MRI or prostate biopsy; (2) receiving radiotherapy, chemotherapy, androgen deprivation therapy, or surgical treatment before mpMRI examination and prostate biopsy; and (3) no signed informed consent.

The primary outcome was the detection rate of csPCa for TB and TB combined with SB histopathological specimens. The reference standard was the pathological results of the combination of TB (AI-cTB or cTB) and SB. Secondary outcomes included (1) the PCa detection rates for TB and TB combined with SB, (2) the Gleason score (GS) of the prostate biopsy sample, (3) the biopsy core positive rate, (4) the largest tumor percentage in all cores of prostate targeted biopsy, and (5) the GS of radical prostatectomy (RP) specimens when conceivable.

Randomization and masking

Eligible patients were randomly allocated at a ratio of 1:1 to a group undergoing AI-cTB plus systematic biopsy (SB) or a group undergoing routine cTB plus SB. Randomization was achieved by using a computer-generated list of random numbers. The list was password-protected in a central database. Patients were allocated by an independent research nurse to ensure that the assigned group could not be predicted.

Sample size

According to previous publications, it was conservatively hypothesized that the csPCa detection rate of cTB combined with SB was 40% [4, 14]. There was no publication on cancer detection rates in biopsy-naïve men undergoing AI-cTB. According to the pre-experimental results for the AI-cTB technique, the expected csPCa detection rate was approximately 55%. At a significance level of 0.05, 340 patients were required to provide 80% power with a two-tailed test for two independent proportions to reveal the previously observed 20% difference between the two groups. To account for potential dropout and the effect of stratification, the sample size was inflated by 10%, resulting in a total of 380 participants.

Prostate biopsy

The biopsy procedure was conducted by a highly skilled and experienced urologist who specializes in performing
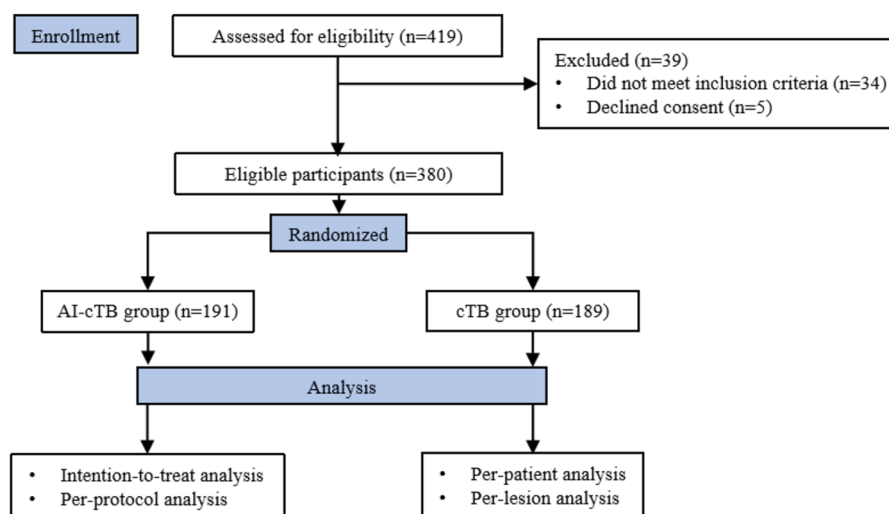

Fig. 1 The flow diagram of the study. Abbreviations: AI-cTB, MRI artificial intelligence-guided cognitive fusion targeted biopsy; cTB, cognitive fusion targeted biopsy

Deng *et al. BMC Medicine*   (2024) 22:530

Page 4 of 13

prostate biopsies. According to the international guideline, prophylactic antibiotics and povidone-iodine were routinely used both before and one day prior to transrectal biopsy, whereas perineal cleaning and antibiotic prophylaxis were conducted before transperineal biopsy [15]. Each patient was placed in the left lateral position or lithotomy position. The ultrasound equipment used included a color Doppler ultrasound diagnostic instrument (Hitachi HiVision, Philips Epiq 7), transrectal probes, and corresponding puncture needle guns. Color Doppler examination was performed from the base to the apex. The prostate volume (PV) was calculated using the following formula: PV (mL) = 0.52 × height (cm) × length (cm) × width (cm). Before proceeding with the biopsy, standard disinfection and draping procedures were carried out to minimize the risk of infection. Then, prostate biopsy was performed under the guidance of an end-fire probe. Prostate biopsies were performed using the transrectal or transperineal route for sampling. The study flowchart is shown in Fig. 2.

Prostate biopsy for the AI-cTB group

The AI software consists of four AI models: (1) MRI sequence classification, (2) prostate gland segmentation and measurement, (3) prostate zonal anatomy segmentation, and (4) csPCa foci segmentation and measurement [16]. The diagnostic accuracy and generalizability of the AI software have been validated in previous publications [12, 13]. Before prostate biopsy, the MR images of patients in the AI-cTB group were uploaded to the AI

software. Then, the AI system automatically segments the whole prostate gland, the anatomic zones, and the csPCa region in a step-by-step manner. A cascade 3D U-Net segmentation framework was used for PCa segmentation [12]. The prostate gland and suspicious lesions were annotated and highlighted by AI software. The urologists who were blinded to the picture archiving and communication system (PACS) and MRI reports read the AI findings at their discretion and then conducted 3–5 core TB procedures at each suspicious lesion, followed by 12 core SB procedures. If there was no suspicious lesion detected by the AI system, only SB was performed.

Prostate biopsy for the cTB group

For patients in the cTB group, the MR images were first evaluated and interpreted according to PI-RADS version 2.1 by urogenital radiologists. The radiologists were blinded to the clinical information of the patients. The radiologists detected and measured the suspected lesions, recorded the location, measured the maximum diameter, and assigned a PI-RADS score to each lesion. Finally, they summarized all the findings and provided a global impression in the reports. The MR images and reports were viewed by urologists preceding the biopsy and were used to cognitively target the MRI-identified lesion using TRUS guidance. If the suspicious lesion was found by urologists from the MR image, three to five targeted biopsies from the lesion were performed by cognitive fusion, followed by 12 core SB. The combination of cTB and SB through fore-zone 12-core biopsy was
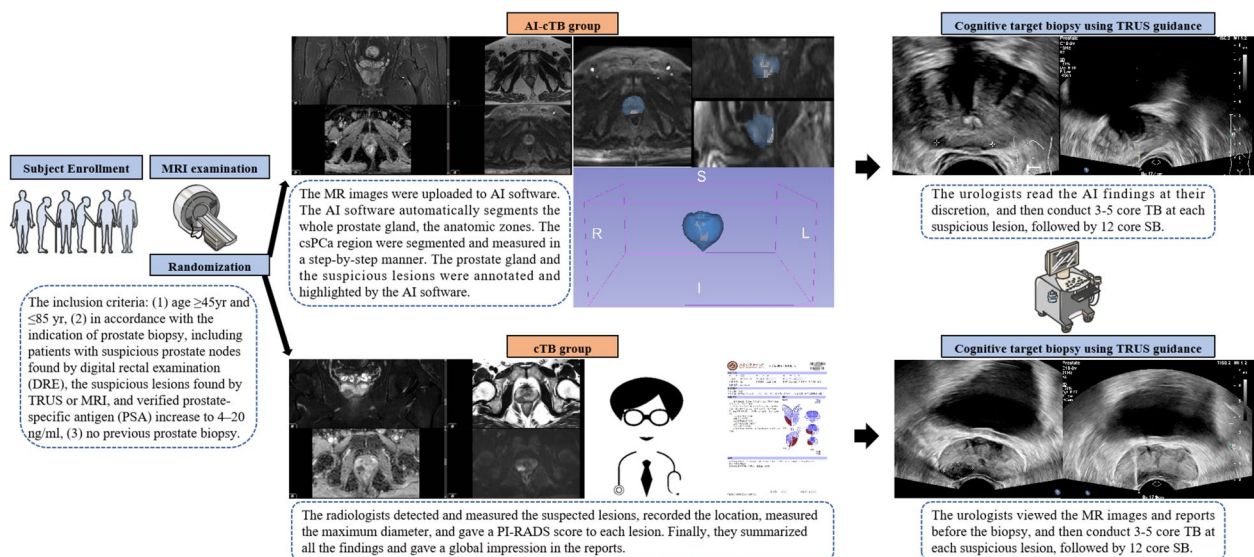
Fig. 2 Study flowchart for AI-cTB versus routine cTB for PCa diagnosis. Abbreviations: AI, artificial intelligence; AI-cTB, MRI artificial intelligence-guided cognitive fusion targeted biopsy; csPCa, clinically significant prostate cancer; cTB, cognitive fusion targeted biopsy; DRE, digital rectal examination; MRI, magnetic resonance imaging; PI-RADS, Prostate Imaging Reporting and Data System; PSA, prostate-specific antigen; SB: systematic biopsy; TB, targeted biopsy; TRUS, transrectal ultrasound

Deng *et al. BMC Medicine*   (2024) 22:530

Page 5 of 13

recommended by the European Association of Urology (EAU) Guidelines. In patients with negative MRI findings, a 12-core SB was performed. When urologists perform biopsies, ultrasound technicians and radiologists will be present to provide necessary assistance.

Pathological evaluation
Each AI-cTB/cTB and SB core was placed in an individual container and reported separately in accordance with the Ginsburg scheme. Histology was evaluated by senior uropathologists who were blinded to the imaging findings. The number of total and positive cores, biopsy Gleason score, grade group, and largest tumor percentage in all cores of each patient were acquired according to the Standards of Reporting for MRI Targeted Biopsy Studies (START) criteria and interpreted according to the recommendations of the International Society of Urological Pathology (ISUP) Grade Group [17, 18]. csPCa was defined as PCa with a grade group (GG) > 2 or GS ≥ 7. For the RP specimens, the overall grade was assigned based on the part with the highest Gleason score according to the recommendations of the ISUP.

Statistical analysis
The demographic and clinical characteristics are summarized as the mean ± SD, the median and IQR, or the frequency, as appropriate. Chi-square or Fisher's exact tests, Student's t tests, and nonparametric tests were used to compare characteristics between patient groups.

The prespecified intention-to-treat (ITT) population for analysis included all participants who underwent randomization. The per-protocol population was divided into groups according to the biopsy scheme actually accepted by the patients. For the primary and secondary outcomes, comparisons of csPCa and PCa rates between groups were performed using the chi-square test or Fisher's exact test at both the patient and lesion levels. Prespecified subgroup analyses were performed according to age strata (45 to 65 years and 65 to 85 years), digital rectal examination (DRE) strata (normal and abnormal), PSA strata (4 to 9.9 and ≥ 10 ng/mL), biopsy route strata (transrectal and transperineal), lesion strata (single lesion and multiple lesion), zone strata (peripheral zone [PZ], transitional zone [TZ], and PZ + TZ), transrectal ultrasound strata (none/benign lesion and malignant lesion), and MRI strata (no and yes). Furthermore, univariate and multivariate logistic regression analyses assessing the associations between pre-biopsy parameters and the detection of csPCa were performed. A priori cutoff p value less than 0.1 for the univariate model was used as the inclusion criterion for multivariate logistic regression analysis.

All the statistical analyses were performed with R statistical software (version 4.3.1; http://www.r-project.org/). A two-sided $p < 0.05$ was considered to indicate statistical significance. Reporting followed the CONSORT statement and the Standards of Reporting of Diagnostic Accuracy [19]. The CONSORT checklist is given in the supplementary material.

Results
Study population
A total of 419 men were enrolled in the study from August 1, 2023, to March 31, 2024, 39 of whom withdrew due to ineligibility or declined consent (Fig. 1). Data were available for 380 patients randomized to the AI-cTB group ($n = 191$) or the cTB group ($n = 189$) (ITT population). Patient pre-biopsy baseline variables were comparable between the two groups (Table 1). The median (interquartile range [IQR]) age of the overall population was 67 [61, 72] years. The median [IQR] PSA concentration was 10.06 ng/ml. Only a small proportion of patients had abnormal DRE results (27.5%). A total of 444 specimens were obtained from 380 patients. The main biopsy route was transrectal (90%). No differences were found in terms of age, DRE results, PSA, PV, PSA density (PSAD), biopsy route, number or distribution of suspected lesions, or transrectal ultrasound results ($p > 0.05$). Protocol violations occurred in 44 patients in the AI-cTB group and 16 patients in the cTB group because the AI system or urologists could not detect suspected lesions from the MR images of these patients. After excluding these patients, 147 and 173 patients were evaluated in the AI-cTB and cTB groups (per-protocol population), respectively.

Outcomes
Primary outcomes
The histopathological characteristics of the ITT population are shown in Table 2. At the patient level, the overall csPCa and PCa detection rates were 58.8% and 61.3%, respectively. The csPCa detection rates of TB combined with SB in the AI-cTB group were significantly greater than those in the cTB group at both the patient level (58.64% vs. 46.56%, $p = 0.018$, Table 3) and per-lesion level (61.47% vs. 47.79%, $p = 0.004$, Table 4). The per-protocol analysis demonstrated that compared with cTB, the AI-cTB could detect a greater proportion of patients with csPCa at both the per-patient level (69.39% vs. 49.71%, $p < 0.001$) and per-lesion level (68.97% vs. 48.57%, $p < 0.001$). Consistently, the rate of csPCa detection of TB combined with SB in the AI-cTB group was significantly greater than that in the cTB group (per-protocol analysis: per-patient level: 71.43% vs. 50.29%, $p < 0.001$; per-lesion level 72.99% vs. 50.95%, $p < 0.001$).

Deng *et al. BMC Medicine*   (2024) 22:530

Page 6 of 13

Table 1 Baseline characteristics of the study populations

Characteristics		Overall (*n* = 380)	AI-cTB group (*n* = 191)	cTB group (*n* = 189)	*p* value
Age (median [IQR])		67.00 [61.00, 72.00]	67.00 [61.00, 73.00]	67.00 [61.00, 72.00]	0.613
DRE (%)	Normal	272 (72.5)	131 (69.3)	141 (75.8)	0.196
	Abnormal	103 (27.5)	58 (30.7)	45 (24.2)	
PSA (median [IQR])		10.06 [7.05, 13.88]	10.17 [7.13, 13.82]	9.99 [7.01, 13.88]	0.818
Prostate volume measured by transrectal ultrasound (median [IQR])		49.00 [36.00, 71.00]	47.90 [37.70, 68.70]	50.00 [33.00, 73.56]	0.873
PSAD (median [IQR])		0.21 [0.14, 0.32]	0.20 [0.12, 0.30]	0.22 [0.15, 0.33]	0.052
Biopsy route (%)	Transperineal	38 (10.0)	17 (8.9)	21 (11.1)	0.584
	Transrectal	342 (90.0)	174 (91.1)	168 (88.9)	
Laterality (%)	Bilateral	36 (11.5)	15 (10.2)	21 (12.7)	0.308
	Left	140 (44.7)	61 (41.5)	79 (47.6)	
	Right	137 (43.8)	71 (48.3)	66 (39.8)	
Zone	PZ	173 (54.1)	77 (52.4)	96 (55.5)	0.655
	TZ	105 (32.8)	48 (32.7)	57 (32.9)	
	PZ + TZ	42 (13.1)	22 (15.0)	20 (11.6)	
Lesion detected by transrectal ultrasound (%)	None/benign lesion	137 (42.8)	54 (36.7)	83 (48.0)	0.056
	Malignant lesion	183 (57.2)	93 (63.3)	90 (52.0)	
Lesion diameter measured by transrectal ultrasound (median [IQR])		1.45 [1.10, 2.00]	1.40 [1.10, 2.00]	1.50 [1.10, 2.05]	0.939
Number of suspected lesions on MR image (%)	0	60 (15.8)	44 (23.0)	16 (8.5)	0.001
	1	248 (65.3)	110 (57.6)	138 (73.0)	
	2	68 (17.9)	35 (18.3)	33 (17.5)	
	3	4 (1.1)	2 (1.0)	2 (1.1)	
PIRADS (%)	1	0 (0)	NA	0 (0)	-
	2	16 (8.5)	NA	16 (8.5)	
	3	55 (29.1)	NA	55 (29.1)	
	4	71 (37.6)	NA	71 (37.6)	
	5	47 (24.9)	NA	47 (24.9)	

Abbreviations: *AI-cTB* MRI artificial intelligence-guided cognitive fusion targeted biopsy, *cTB* cognitive fusion targeted biopsy, *DRE* digital rectal examination, *IQR* interquartile range, *MRI* magnetic resonance imaging, *PI-RADS* Prostate Imaging Reporting and Data System, *PSA* prostate-specific antigen, *PSAD* prostate-specific antigen density, *PZ* peripheral zone, *TZ* transitional zone

Secondary outcomes

In the ITT population, the PCa detection rate of TB combined with SB was slightly greater in the AI-cTB group than in the cTB group (per-patient level: 64.92% vs. 57.67%, $p = 0.147$; per-lesion level: 67.43% vs. 60.18%, $p = 0.112$). However, in the per-protocol analysis, the PCa detection rate of TB combined with SB in the AI-cTB group was significantly greater than that in the cTB group at both levels ($p < 0.05$). The distribution of ISUP in biopsy specimens in the two groups was significantly different ($p < 0.001$, Fig. 3 and Table 2). The proportion of clinically insignificant PCa (GS = 3 + 3, ISUP 1) was lower in the AI-cTB group than in the cTB group (6.3% vs. 11.1%). However, the distribution of ISUP in RP specimens was similar between the two groups ($p = 0.969$, Fig. 3c). There was no significant difference in the upgrade rate of ISUP after RP between the two groups ($p = 0.522$).

Subgroup analysis

The results of the prespecified subgroup analyses are shown in Tables S1-S2. The AI-cTB exhibited the advantage of accurately detecting csPCa in almost all subgroups ($p < 0.05$). The csPCa and PCa detection rates of TB were significantly greater in the AI-cTB group than in the cTB group among 45- to 65-year-old patients and patients with normal DRE results, PSA levels of 4–10, transrectal biopsy results, single MRI-suspected lesions, suspected lesions located in the TZ, and nonmalignant lesions detected by TRUS ($p < 0.05$, Table S1-S2).

Logistic regression analysis

As shown in Table 5, the univariate logistic regression analysis revealed that age, DRE, PSA level, prostate volume, TB method, suspected lesion location, and ultrasound results were potential factors for detecting csPCa ($p < 0.05$). Further multivariate analysis indicated that older age,

Deng *et al. BMC Medicine*   (2024) 22:530

Page 7 of 13

Table 2 Histopathological characteristics of the study populations

Characteristics		Overall (n = 380)	AI-cTB group (n = 191)	cTB group (n = 189)	*p* value
Positive rate of biopsy cores (median [IQR])		0.25 [0.00, 0.56]	0.33 [0.00, 0.57]	0.20 [0.00, 0.54]	0.094
Maximum cancer core invasion (median [IQR])		80.00 [60.00, 90.00]	80.00 [60.00, 90.00]	80.00 [50.00, 90.00]	0.669
Detection of PCa at TB only, number (%)	No	107 (33.4)	37 (25.2)	70 (40.5)	**0.006**
	Yes	213 (66.6)	110 (74.8)	103 (59.5)	
Detection of PCa TB combined with SB, number (%)	No	147 (38.7)	67 (35.1)	80 (42.3)	0.178
	Yes	233 (61.3)	124 (64.9)	109 (57.7)	
Detection of csPCa at TB only, number (%)	No	132 (41.2)	45 (30.6)	87 (50.3)	**0.001**
	Yes	188 (58.8)	102 (69.4)	86 (49.7)	
Detection of csPCa TB combined with SB, number (%)	No	180 (47.4)	79 (41.4)	101 (53.4)	**0.024**
	Yes	200 (52.6)	112 (58.6)	88 (46.6)	
ISUP of biopsy specimens, number (%)	No PCa	147 (38.7)	67 (35.1)	80 (42.3)	**< 0.001**
	1	33 (8.7)	12 (6.3)	21 (11.1)	
	2	87 (22.9)	61 (31.9)	26 (13.8)	
	3	59 (15.5)	22 (11.5)	37 (19.6)	
	4	23 (6.1)	14 (7.3)	9 (4.8)	
	5	31 (8.2)	15 (7.9)	16 (8.5)	
ISUP of RP specimens, number (%)	1	2 (2.9)	1 (2.6)	1 (3.3)	0.969
	2	40 (58.0)	24 (61.5)	16 (53.3)	
	3	14 (20.3)	7 (17.9)	7 (23.3)	
	4	4 (5.8)	2 (5.1)	2 (6.7)	
	5	9 (13.0)	5 (12.8)	4 (13.3)	
Upgrade of ISUP after RP, number (%)	No	49 (71.0)	26 (66.7)	23 (76.7)	0.522
	Yes	20 (29.0)	13 (33.3)	7 (23.3)	

Abbreviations: *AI-cTB,* MRI artificial intelligence-guided cognitive fusion targeted biopsy, *csPCa* clinically significant prostate cancer, *cTB* cognitive fusion targeted biopsy, *IQR* interquartile range, *ISUP* International Society of Urological Pathology, *PCa* prostate cancer, *RP* radical prostatectomy, *SB* systematic biopsy, *TB* targeted biopsy

Table 3 Comparison of the csPCa detection and PCa detection rates at the patient level

	Overall	AI-cTB group	cTB group	*p* value
Overall detection rate of csPCa at TB combined with SB, % (number/total number)[a]	52.63% (200/380)	58.64% (112/191)	46.56% (88/189)	**0.018**
Overall detection rate of PCa at TB combined with SB, % (number/total number)[a]	61.32% (233/380)	64.92% (124/191)	57.67% (109/189)	0.147
Ratio of overall detection of csPCa/PCa at TB combined with SB, %[a]	85.84% (200/233)	90.32% (112/124)	80.73% (88/109)	0.404
Overall detection rate of csPCa at TB combined with SB, % (number/total number)[b]	60.00% (192/320)	71.43% (105/147)	50.29% (87/173)	**< 0.001**
Overall detection rate of PCa at TB combined with SB, % (number/total number)[b]	61.32% (222/320)	77.55% (114/147)	62.43% (108/173)	**0.003**
Ratio of overall detection of csPCa/PCa at TB combined with SB, %[b]	86.48% (192/222)	92.10% (105/114)	80.56% (87/108)	**0.005**
Overall detection rate of csPCa at TB only, % (number/total number)[b]	58.75% (188/320)	69.39% (102/147)	49.71% (86/173)	**< 0.001**
Overall detection rate of PCa at TB only, % (number/total number)[b]	66.56% (213/320)	74.83% (110/147)	59.54% (103/173)	**0.004**
Ratio of overall detection of csPCa/PCa at TB, %[b]	88.26% (188/213)	92.72% (102/110)	83.50% (86/103)	**0.006**

Abbreviations: *AI-cTB* MRI artificial intelligence-guided cognitive fusion targeted biopsy, *csPCa* clinically significant prostate cancer, *cTB* cognitive fusion targeted biopsy, *SB* systematic biopsy, *TB* targeted biopsy

[a] Intention-to-treat analysis

[b] Per-protocol analysis

abnormal DRE results, higher PSA levels, TB methods, and malignant lesions detected by ultrasound were significantly associated with the detection of csPCa ($p < 0.05$). Notably, compared with cTB, the AI-cTB significantly improved the possibility of detecting csPCa (OR = 2.93, 95% confidence interval [CI]: 1.61–5.49, $p < 0.001$; Table 5).

Deng *et al. BMC Medicine*   (2024) 22:530

Page 8 of 13

Table 4 Comparison of the csPCa detection and PCa detection rates at the lesion level

	Overall	AI-cTB group	cTB group	*p* value
Overall detection rate of csPCa at TB combined with SB, % (number/total number)[a]	54.50% (242/444)	61.47% (134/218)	47.79% (108/226)	**0.004**
Overall detection rate of PCa at TB combined with SB, % (number/total number)[a]	63.74% (283/444)	67.43% (147/218)	60.18% (136/226)	0.112
Ratio of overall detection of csPCa/PCa at TB combined with SB, %[a]	85.51% (242/283)	91.28% (134/147)	79.56% (108/136)	0.141
Overall detection rate of csPCa at TB combined with SB, % (number/total number)[b]	60.94% (234/384)	72.99% (127/174)	50.95% (107/210)	**< 0.001**
Overall detection rate of PCa at TB combined with SB, % (number/total number)[b]	70.83% (272/384)	78.74% (137/174)	64.29% (135/210)	**0.002**
Ratio of overall detection of csPCa/PCa at TB combined with SB, %[b]	85.51% (234/272)	92.70% (127/137)	79.26% (107/135)	**0.002**
Overall detection rate of csPCa at TB only, % (number/total number)[b]	57.81% (222/384)	68.97% (120/174)	48.57% (102/210)	**< 0.001**
Overall detection rate of PCa at TB only, % (number/total number)[b]	65.10% (250/384)	74.14% (129/174)	57.62% (121/210)	**0.001**
Ratio of overall detection of csPCa/PCa at TB, %[b]	88.80% (222/250)	93.02% (120/129)	84.30% (102/121)	**0.008**

Abbreviations: *AI-cTB*, MRI artificial intelligence-guided cognitive fusion targeted biopsy, *csPCa* clinically significant prostate cancer, *cTB* cognitive fusion targeted biopsy, *SB* systematic biopsy, *TB* targeted biopsy

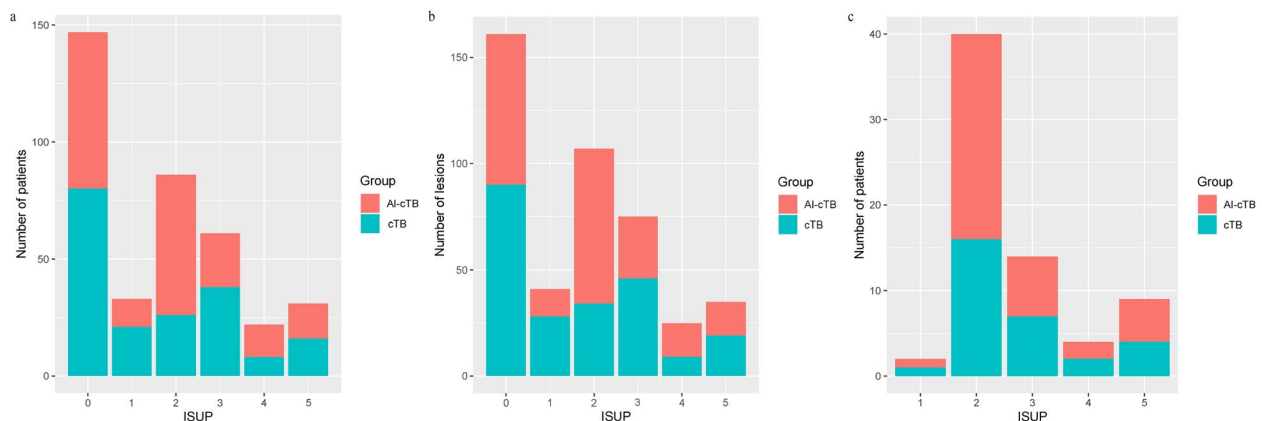[a] Intention-to-treat analysis

[b] Per-protocol analysis

Fig. 3 Histogram of ISUP. **a** ISUP of patient biopsy specimens (*n* = 380). **b** ISUP of lesion biopsy specimens (*n* = 444). **c** ISUP of RP specimens (*n* = 69). Abbreviations: AI-cTB, MRI artificial intelligence-guided cognitive fusion targeted biopsy; cTB, cognitive fusion targeted biopsy; ISUP, International Society of Urological Pathology; RP, radical prostatectomy

Discussion

To the best of our knowledge, this is the first RCT to investigate the application of AI in assisting prostate TB. Motivated by the rapid development of AI in the medical field, we realized that AI has the potential to revolutionize current clinical practice. However, AI has not yet been fully integrated into clinical practice. There is still a lack of high-quality prospective clinical trials demonstrating the clinical application value of AI in assisting prostate diagnosis [5]. Therefore, we designed this RCT to explore the clinical utility value of AI in prostate biopsy with the aim of promoting the accurate diagnosis and individualized treatment of prostate cancer. This RCT was designed in accordance with good clinical practice guidelines and followed the concept of precision medicine [20]. This study demonstrated that the AI-cTB significantly improved the detection rate of csPCa for TB and TB combined with SB. The secondary outcomes showed

that the AI-cTB could increase PCa detection rates and decrease the detection of clinically insignificant PCa.

With the development of new technologies such as mpMRI, several image-guided prostate biopsy techniques have emerged [3]. When suspicious lesions are detected on prostate MR images, TB of the lesions can be detected by several methods, including cTB, MRI-TB, and FUS-TB, which can all be performed via either the transrectal or transperineal route [14]. MRI-TB is conducted within an MRI scanner using real-time MRI guidance. Using dedicated software that performs MR and TRUS image fusion, FUS-TB could be constructed under fusion image guidance [14]. However, due to the high technology costs and limited availability of these systems, widespread diffusion of MRI-TB and FUS-TB has yet to be achieved in urology departments [4]. Image fusion platforms have additional costs and may malfunction, and extra steps, such as image acquisition

Deng *et al. BMC Medicine*   (2024) 22:530

Page 9 of 13

Table 5 Univariate and multivariate logistic analyses for the detection of csPCa

Characteristics		Univariate analysis			Multivariate analysis		
		OR	95% CI	*p* value	OR	95% CI	*p* value
Age		1.05	1.02–1.09	**< 0.001**	1.07	1.02–1.12	**0.007**
DRE	Normal	Reference			Reference		
	Abnormal	6.16	3.34–11.34	**< 0.001**	3.42	1.65–7.40	**0.001**
PSA		1.07	1.02–1.12	**0.010**	1.11	1.04–1.19	**0.002**
Prostate volume measured by ultrasound		0.98	0.97–0.99	**< 0.001**	0.97	0.96–0.98	**< 0.001**
TB	cTB	Reference			Reference		
	AI-cTB	2.29	1.45–3.63	**< 0.001**	2.93	1.61–5.49	**< 0.001**
Number of suspected lesions detected by MRI	1	Reference					
	>1	1.43	0.83–2.46	0.2			
Laterality	Left	Reference			Reference		
	Right	0.91	0.56–1.46	0.69	2.43	0.51–1.82	0.913
	Bilateral	2.55	1.08–5.99	**0.03**	0.97	0.82–7.89	0.122
Zone	PZ	Reference			Reference		
	TZ	0.3	0.18–0.49	**< 0.001**	0.48	0.24–0.95	**0.035**
	PZ+TZ	2.14	0.93–4.93	0.07	1.66	0.62–4.87	0.326
Suspected lesion detected by ultrasound	None/benign lesion	Reference			Reference		
	Malignant lesion	8.93	5.35–14.89	**< 0.001**	3.92	2.08–7.48	**< 0.001**

Abbreviations: *AI-cTB* MRI artificial intelligence-guided cognitive fusion targeted biopsy, *csPCa* clinically significant prostate cancer, *cTB* cognitive fusion targeted biopsy, *DRE* digital rectal examination, *MRI* magnetic resonance imaging, *PSA* prostate-specific antigen, *PZ* peripheral zone *TB* targeted biopsy *TZ* transitional zone

and contouring, could lengthen the procedure duration [21]. cTB does not require any additional equipment and has been widely used. The operators could cognitively sample the prostate through TRUS with the aid of the visual map provided by MRI imaging via visual image alignment [4]. However, it relies heavily on the operator's intuitiveness, experience, and confidence in MRI reading, and varying levels of operator experience can lead to inter-operator variability [4]. For cTB, the operator's confidence in MRI readings should be high to enable adequate cognitive biopsies [4]. It is especially relevant for young urologists, as previous surveys have identified important knowledge gaps and a lack of confidence in MRI readings and interpretations worldwide [4, 22]. Various previous studies have demonstrated that there was no significant difference in cancer detection rates among the three TB methods [3, 4, 14]. The role of prostate biopsy has undergone significant changes. The significance of prostate biopsy has evolved from pure detection of any PCa to better characterization of csPCa to assist in the clinical management of patients [23]. Accurate characterization and three-dimensional localization of csPCa are crucial for diagnosing the disease and devising effective treatment strategies. The schemes for prostate biopsy warrant further optimization.

In recent years, new breakthroughs in AI have provided new network models with the powerful ability to identify the deep features of medical images and combine multiple imaging modalities and multiple time points, allowing AI to more fully and accurately characterize tumor heterogeneity [6]. Applying AI in clinical practice could be considered a low-cost value-added activity if it could greatly improve the efficiency and accuracy of PCa diagnosis [8]. However, some current AI models are plagued with disadvantages such as biases due to limited training data from single centers, lack of strict external and independent cohorts, and inability to use human-like diagnostic interpretive tools. The AI software used in this RCT was trained using MR images from three hospitals and validated with sixteen radiologists from four hospitals; the results showed strong robustness, high reliability, and generalizability [13]. Based on high-quality real-world datasets from multiple centers, AI software could not only improve the diagnostic accuracy of PCa and reduce inter-reader variability but also shorten the mean reporting time and improve efficiency in clinical practice [13]. In this RCT, we further integrated it with prostate biopsy. The population baseline characteristics were balanced except for number of suspected lesions on MR images, which may be due to the different criteria for interpreting MR images between radiologists

Deng *et al. BMC Medicine*   (2024) 22:530

Page 10 of 13

and AI. It would not have a substantial impact on overall results. The detection rates of csPCa with the AI-cTB combined with SB reached 58.64% according to the ITT analysis and 77.55% according to the per-protocol analysis, which were significantly greater than the csPCa detection rates with the cTB combined with SB reported in previous studies (mostly 30%-50%) [24–26]. The percentage of positive biopsy cores in the AI-cTB group was also greater than that in the cTB group (median: 33% vs. 20%). Recently, another RCT investigated the application of AI ultrasound of prostate (AIUSP)-targeted biopsy in PCa diagnosis. The csPCa detection rate was 32.3% in the AIUSP group, and the overall percentage of positive biopsy cores was 22.7% [27], which was lower than that in this study. The superiority of the AI-cTB in accurately diagnosing csPCa was validated in different populations (the ITT population and per-protocol population) at multiple levels (per-patient level and per-lesion level). Multivariate logistic analysis also showed that the AI-cTB could significantly improve the possibility of detecting csPCa. In addition, to comprehensively evaluate the application value of the AI-cTB, we conducted a subgroup analysis according to characteristic strata. The superiority of the AI-cTB mainly appears in the subgroups containing patients who did not have typical clinical manifestations or tumor characteristics. For example, the AI-cTB significantly increased the csPCa detection rate among patients with normal DRE results but not among patients with abnormal DRE results. The targeted biopsy detection rates for PCa and csPCa located in peripheral zone (PZ) was significantly higher than lesions located in transitional zone (TZ) in this study (PCa: 79.19% vs 66.53%, csPCa: 66.47% vs 37.14%, $p < 0.05$). PCa usually occurs in the PZ of the prostate. Suspicious areas in PZ of the prostate often appear hypointense compared to the healthy glandular tissue, which was relatively easy to detect. However, TZ is often hypointense on T2WI, so PCa is more difficult to identify. Suspicious lesions here are characterized by ill-defined edges, with an "erased charcoal" appearance, and sometimes they may have a spiculated or water-drop appearance [28]. The subgroup analysis indicated that the AI-cTB was superior to cTB only among patients with PCa located in the TZ. In addition, if malignant lesions were detected via TRUS, the csPCa detection rate of the AI-cTB would be slightly greater than that of the cTB. However, the AI-cTB could significantly increase the csPCa detection rate when TRUS did not detect suspicious lesions or detected only benign lesions. In brief, the above results demonstrated the powerful ability of the AI-cTB to diagnose PCa, which is atypical or difficult to detect. The good performance of the AI-cTB when facing tumor heterogeneity is mainly attributed to large-scale diverse multicenter training [5]. Furthermore, detecting and subsequent treatment of clinically insignificant PCa would not improve life expectancy but would expose patients to unnecessary side effects and incur health care costs [29]. AI-cTB detected less clinically insignificant PCa than did cTB (6.3% vs. 11.1%), exhibiting the ability to reduce overtreatment and improve safety. However, the distributions of the ISUP in the RP specimens and the upgrade rates between the two groups were similar. We supposed that PCa patients who underwent RP were strictly screened and evaluated by multiple examinations, thus leading to similar pathological outcomes after RP.

The strengths of this study included a head-to-head comparison between AI-cTB and traditional cTB. The prospective RCT design minimized bias and led to balanced baseline characteristics, increasing the reliability of the results. Compared with other types of fusion TB, the AI-cTB could greatly avoid unnecessary biopsies and help urologists achieve a precise diagnosis of csPCa. Traditional cTB requires constant accumulation of experience and is limited by its high level of expertise, time, and cost [27]. Conversely, the AI-cTB is associated with greater inter-operator consistency and a more favorable learning curve, which makes it easy to generalize. The AI-cTB has the potential to reduce medical expenses on a national economic scale by promoting precise health care and improving labor time efficiency [30]. We successfully integrated AI with TB to allow clinical use in real-world healthcare settings and provided a research paradigm for integrating AI into prospective clinical studies.

Although the current results on the AI-cTB are promising, there are some limitations in this study. First, this was a single-center RCT, and all biopsies were performed by experienced urologists, thus limiting the generalizability of the results with respect to less experienced urologists. These results require external validation and further confirmation in future multicenter studies. Interinstitutional and multidisciplinary collaboration are crucial for the routine development of reliable and accountable AI technology in clinical practice [31]. Second, the sample size was calculated based on primary outcomes. Secondary outcomes may be partially affected by the sample size, so these outcomes should be explained considering this issue. Further studies are warranted to evaluate these secondary outcomes. Furthermore, only 69 patients (18.2%) underwent RP. The relatively low sample size might not have enough statistical power to analyze pathological outcomes after RP, such as histological upgrading and downgrading.

This study did not involve prostate-specific membrane antigen (PSMA) positron emission tomography (PET) and computed tomography (CT). In recent years, the development of PSMA PET CT scan has improved

Deng *et al. BMC Medicine* (2024) 22:530

Page 11 of 13

the diagnosis of PCa [32]. PSMA PET CT scan has performed unique advantages in the detection of metastatic and recurrent lesions of PCa [33–35]. However, its power in diagnosing primary lesions of prostate cancer still needs to be proven. There are several reasons for this. First, the spatial resolution of the PET scan is still not accurate enough for clinical tumor staging. Second, the resolution ability of CT examination is limited for prostate soft tissue. Third, it is difficult to clearly distinguish prostatitis and prostate cancer. What is more, considering health economics, the PSMA PET CT scan is difficult to be accepted by most patients as a routine examination [35]. Therefore, we did not routinely conduct PSMA PET CT examination for patients in this study. In the future study, we would try to investigate the role of PSMA PET CT in the diagnosis of PCa and developed AI for PSMA PET CT.

Finally, the main biopsy route in this study was transrectal (90.0%). The recent international guidelines recommended the transperineal prostate biopsy because of its relatively lower risk of biopsy-related infections and its advantage for detecting anterior PCa [1, 36, 37]. A meta-analysis of eleven RCTs including 2237 men demonstrated that the use of rectal povidone-iodine preparation before biopsy and antimicrobial prophylaxis resulted in a significantly lower rate of infectious complications [38]. According to the international guideline recommendations, subjects in this study conducted rectal povidone-iodine preparation and accepted routine prophylactic antibiotics treatment prior to transrectal prostate biopsy [15]. Actually, the rate of biopsy-related infections was low in this study, and there was no significant difference between patients receiving transrectal biopsy with targeted antibiotic prophylaxis and those receiving transperineal biopsy (2.92% vs 2.63%, $p > 0.05$), which was consistent with previous studies [39, 40]. Regarding PCa detection rate, though transperineal biopsy may be superior for detection of PCa tumor located in the anterior area, previous studies indicated that there was no significant statistical difference in overall PCa detection between the two approaches [41, 42]. The AI-cTB did not exhibit superiority in the subgroup of patients who underwent transperineal prostate biopsy, which may attribute to the small sample size of patients receiving transperineal biopsy and relatively low statistical efficiency. Therefore, in the current study, the choice between transrectal cTB and transperineal cTB was not expected to have a substantial impact on the overall results. In the future, we would further investigate the role of AI-cTB through transperineal approach in diagnosing PCa.

Conclusions

In summary, the AI-cTB may effectively improve the detection rate of csPCa. We successfully integrated AI with TB in a routine clinical workflow and provided a research paradigm for prospective AI-integrated clinical studies. Further advancement in the management of PCa requires the establishment of a computation-to-clinic synergy [30]. AI should further extend to fields beyond the diagnosis of PCa, such as the prediction of prognosis, local recurrence, risk stratification, and individualized treatment, ultimately optimizing comprehensive management of PCa and promoting the development of precision medicine.

Abbreviations

AI	Artificial intelligence
AI-cTB	MRI artificial intelligence-guided cognitive fusion MRI-guided targeted biopsy
AIUSP	Artificial intelligence ultrasound of prostate
csPCa	Clinically significant prostate cancer
cTB	Cognitive fusion MRI-guided targeted biopsy
DRE	Digital rectal examination
EAU	European Association of Urology
GG	Grade group
GS	Gleason score
ISUP	International Society of Urological Pathology
IQR	Interquartile range
ITT	Intention-to-treat
mpMRI	Multiparametric magnetic resonance imaging
MRI-TB	In-bore MRI target biopsy
PCa	Prostate cancer
PCAS	Picture archiving and communication system
PSA	Prostate-specific antigen
PSAD	Prostate-specific antigen density
PV	Prostate volume
PZ	Peripheral zone
RCT	Randomized controlled trial
RP	Radical prostatectomy
SB	Systematic biopsy
START	Standards of Reporting for MRI Targeted Biopsy Studies
TRUS	MRI-transrectal ultrasound
TZ	Transitional zone

Supplementary Information

The online version contains supplementary material available at https://doi.org/10.1186/s12916-024-03742-z.

> Additional file 1. Tables S1-S2. Tables S1-Stratified comparison of csPCa detection and PCa detection rates at the patient level. Tables S2- Stratified comparison of csPCa detection and PCa detection rates at the per-lesion level.

Authors' contributions

R.D. and Y.L. were involved in the study design, conducted the data analyses, and wrote the first draft of the manuscript. X.W. and K.G. conceptualized this trial, contributed to the interpretation of results, and reviewed and substantially revised the manuscript. K.W., M.R., D.L., J.W., J.Q., P.T., C.Y., J.S., Z.Z., J.Z., L.C., participated in acquisition, analysis, and interpretation of data. P.W. developed and ran the MRI-AI software. All authors read and approved the final manuscript.

Deng *et al. BMC Medicine*   (2024) 22:530

Page 12 of 13

Data availability

No datasets were generated or analysed during the current study.

Declarations

Ethics approval and consent to participate

The study was reviewed and approved by the institutional review board of Peking University First Hospital (2023IR27).

Consent for publication

Not applicable.

Competing interests

The authors declare no competing interests.

Author details

[1]Department of Urology, Peking University First Hospital, Beijing, China. [2]Institute of Urology, Peking University, Beijing, China. [3]National Urological Cancer Center, Beijing, China. [4]School of Basic Medical Sciences, Capital Medical University, Beijing, China. [5]Beijing Smart Tree Medical Technology Co. Ltd, Beijing, China. [6]Department of Radiology, Peking University First Hospital, Beijing, China.

References

1. Mottet N, van den Bergh RCN, Briers E, Van den Broeck T, Cumberbatch MG, De Santis M, et al. EAU-EANM-ESTRO-ESUR-SIOG guidelines on prostate cancer-2020 update. Part 1: screening, diagnosis, and local treatment with curative intent. Eur Urol. 2021;79(2):243–62.
2. Lorusso V, Kabre B, Pignot G, Branger N, Pacchetti A, Thomassin-Piana J, et al. External validation of the computerized analysis of TRUS of the prostate with the ANNA/C-TRUS system: a potential role of artificial intelligence for improving prostate cancer detection. World J Urol. 2023;41(3):619–25.
3. Wegelin O, van Melick HHE, Hooft L, Bosch JLHR, Reitsma HB, Barentsz JO, et al. Comparing three different techniques for magnetic resonance imaging-targeted prostate biopsies: a systematic review of in-bore versus magnetic resonance imaging-transrectal ultrasound fusion versus cognitive registration. Is there a preferred technique? Eur Urol. 2017;71(4):517–31.
4. Pirola GM, Castellani D, Orecchia L, Giulioni C, Gubbiotti M, Rubilotta E, et al. Transperineal US-MRI fusion-guided biopsy for the detection of clinical significant prostate cancer: a systematic review and meta-analysis comparing cognitive and software-assisted technique. Cancers (Basel). 2023;30;15(13):3443.
5. Turkbey B, Haider MA. Artificial intelligence for automated cancer detection on prostate MRI: opportunities and ongoing challenges, from the AJR Special Series on AI Applications. AJR Am J Roentgenol. 2022;219(2):188–94.
6. Zhao LT, Liu ZY, Xie WF, Shao LZ, Lu J, Tian J, et al. What benefit can be obtained from magnetic resonance imaging diagnosis with artificial intelligence in prostate cancer compared with clinical assessments? Mil Med Res. 2023;10(1):29.
7. Labus S, Altmann MM, Huisman H, Tong A, Penzkofer T, Choi MH, et al. A concurrent, deep learning-based computer-aided detection system for prostate multiparametric MRI: a performance study involving experienced and less-experienced radiologists. Eur Radiol. 2023;33(1):64–76.
8. Sun YK, Zhou BY, Miao Y, Shi YL, Xu SH, Wu DM, et al. Three-dimensional convolutional neural network model to identify clinically significant prostate cancer in transrectal ultrasound videos: a prospective, multi-institutional, diagnostic study. EClinicalMedicine. 2023;60: 102027.
9. Thomas M, Murali S, Simpson BSS, Freeman A, Kirkham A, Kelly D, et al. Use of artificial intelligence in the detection of primary prostate cancer in multiparametric MRI with its clinical outcomes: a protocol for a systematic review and meta-analysis. BMJ Open. 2023;22;13(8):e074009.
10. Hiremath A, Shiradkar R, Fu P, Mahran A, Rastinehad AR, Tewari A, et al. An integrated nomogram combining deep learning, Prostate Imaging-Reporting and Data System (PI-RADS) scoring, and clinical variables for identification of clinically significant prostate cancer on biparametric MRI: a retrospective multicentre study. Lancet Digit Health. 2021;3(7):e445–54.
11. Zhao L, Bao J, Qiao X, Jin P, et al. Predicting clinically significant prostate cancer with a deep learning approach: a multicentre retrospective study. Eur J Nucl Med Mol Imaging. 2023;50(3):727–41.
12. Sun Z, Wu P, Cui Y, Liu X, Wang K, Gao G, et al. Deep-learning models for detection and localization of visible clinically significant prostate cancer on multi-parametric MRI. J Magn Reson Imaging. 2023;58(4):1067–81.
13. Sun Z, Wang K, Kong Z, Xing Z, Chen Y, Luo N, et al. A multicenter study of artificial intelligence-aided software for detecting visible clinically significant prostate cancer on mpMRI. Insights Imaging. 2023;14(1):72.
14. Watts KL, Frechette L, Muller B, Ilinksy D, Kovac E, Sankin A, et al. Systematic review and meta-analysis comparing cognitive vs. image-guided fusion prostate biopsy for the detection of prostate cancer. Urol Oncol. 2020;38(9):734.e19–734.e25.
15. Cornford P, van den Bergh RCN, Briers E, Van den Broeck T, Brunckhorst O, Darraugh J, et al. EAU-EANM-ESTRO-ESUR-ISUP-SIOG guidelines on prostate cancer-2024 update. part i: screening, diagnosis, and local treatment with curative intent. Eur Urol. 2024;86(2):148–63.
16. Zhu Y, Wei R, Gao G, Ding L, Zhang X, Wang X, et al. Fully automatic segmentation on prostate MR images based on cascaded fully convolution network. J Magn Reson Imaging. 2019;49(4):1149–56.
17. Moore CM, Kasivisvanathan V, Eggener S, Emberton M, Fütterer JJ, Gill IS, et al. Standards of reporting for MRI-targeted biopsy studies (START) of the prostate: recommendations from an International Working Group. Eur Urol. 2013;64(4):544–52.
18. Epstein JI, Egevad L, Amin MB, Delahunt B, Srigley JR, Humphrey PA, et al. The 2014 International Society of Urological Pathology (ISUP) consensus conference on Gleason grading of prostatic carcinoma: definition of grading patterns and proposal for a new grading system. Am J Surg Pathol. 2016;40(2):244–52.
19. Bossuyt PM, Reitsma JB, Bruns DE, Gatsonis CA, Glasziou PP, Irwig LM, et al. Towards complete and accurate reporting of studies of diagnostic accuracy: The STARD Initiative. Radiology. 2003;226(1):24–8.
20. Checcucci E, Amparore D, De Luca S, Autorino R, Fiori C, Porpiglia F. Precision prostate cancer surgery: an overview of new technologies and techniques. Minerva Urol Nefrol. 2019;71(5):487–501.
21. Khoo CC, Eldred-Evans D, Peters M, van Son M, van Rossum PSN, Connor MJ, et al. A comparison of prostate cancer detection between visual estimation (cognitive registration) and image fusion (software registration) targeted transperineal prostate biopsy. J Urol. 2021;205(4):1075–81.
22. Ippoliti S, Orecchia L, Esperto F, Langer Wroclawski M, Manenti G, Barrett T, et al. Survey on prostate MRI reading and interpretation among urology residents in Italy, Brazil and the UK: a cry for help. Minerva Urol Nephrol. 2023;75(3):297–307.
23. Connor MJ, Gorin MA, Eldred-Evans D, Bass EJ, Desai A, Dudderidge T, et al. Landmarks in the evolution of prostate biopsy. Nat Rev Urol. 2023;20(4):241–58.
24. Hamid S, Donaldson IA, Hu Y, Rodell R, Villarini B, Bonmati E, et al. The SmartTarget biopsy trial: a prospective, within-person randomised, blinded trial comparing the accuracy of visual-registration and magnetic resonance imaging/ultrasound image-fusion targeted biopsies for prostate cancer risk stratification. Eur Urol. 2019;75(5):733–40.
25. Liang L, Cheng Y, Qi F, Zhang L, Cao D, Cheng G, et al. A comparative study of prostate cancer detection rate between transperineal COG-TB and transperineal FUS-TB in patients with PSA ≤20 ng/mL. J Endourol. 2020;34(10):1008–14.

Deng *et al. BMC Medicine*   (2024) 22:530

Page 13 of 13

26. Izadpanahi MH, Elahian A, Gholipour F, Khorrami MH, Zargham M, Mohammadi Sichani M, et al. Diagnostic yield of fusion magnetic resonance-guided prostate biopsy versus cognitive-guided biopsy in biopsy-naive patients: a head-to-head randomized controlled trial. Prostate Cancer Prostatic Dis. 2021;24(4):1103–9.

27. Wang X, Xie Y, Zheng X, Liu B, Chen H, Li J, et al. A prospective multicenter randomized comparative trial evaluating outcomes of transrectal ultrasound (TRUS)-guided 12-core systematic biopsy, mpMRI-targeted 12-core biopsy, and artificial intelligence ultrasound of prostate (AIUSP) 6-core targeted biopsy for prostate cancer diagnosis. World J Urol. 2023;41(3):653–62.

28. Teică RV, Șerbănescu MS, Florescu LM, Gheonea IA. Tumor area highlighting using T2WI, ADC map, and DWI sequence fusion on bpMRI images for better prostate cancer diagnosis. Life (Basel). 2023; 30;13(4):910.

29. Schröder FH, Hugosson J, Roobol MJ, Tammela TLJ, Ciatto S, Nelen V, et al. Prostate-cancer mortality at 11 years of follow-up. N Engl J Med. 2012;366(11):981–90.

30. Baydoun A, Jia AY, Zaorsky NG, Kashani R, Rao S, Shoag JE, et al. Artificial intelligence applications in prostate cancer. Prostate Cancer Prostatic Dis. 2024;27(1):37–45.

31. Kartasalo K, Bulten W, Delahunt B, et al. Artificial intelligence for diagnosis and Gleason grading of prostate cancer in biopsies-current status and next steps. Eur Urol Focus. 2021;7(4):687–91.

32. Pepe P, Pepe L, Cosentino S, Ippolito M, Pennisi M, Fraggetta F. Detection rate of 68Ga-PSMA PET/CT vs. mpMRI targeted biopsy for clinically significant prostate cancer. Anticancer Res. 2022;42(6):3011–5.

33. Lombardo R, Tema G, Nacchia A, Mancini E, Franco S, Zammitti F, et al. Role of perilesional sampling of patients undergoing fusion prostate biopsies. Life (Basel). 2023;13(8):1719.

34. Pepe P, Pennisi M. Targeted biopsy in men high risk for prostate cancer: 68Ga-PSMA PET/CT versus mpMRI. Clin Genitourin Cancer. 2023;21(6):639–42.

35. Qiu DX, Li J, Zhang JW, Chen MF, Gao XM, Tang YX, et al. Dual-tracer PET/CT-targeted, mpMRI-targeted, systematic biopsy, and combined biopsy for the diagnosis of prostate cancer: a pilot study. Eur J Nucl Med Mol Imaging. 2022;49(8):2821–32.

36. Pepe P, Pennisi M. Morbidity following transperineal prostate biopsy: our experience in 8.500 men. Arch Ital Urol Androl. 2022;94(2):155–9.

37. Pepe P, Fandella A, Barbera M, Martino P, Merolla F, Caputo A, et al. Advances in radiology and pathology of prostate cancer: a review for the pathologist. Pathologica. 2024;116(1):1–12.

38. Pradere B, Veeratterapillay R, Dimitropoulos K, Yuan Y, Omar MI, MacLennan S, et al. Nonantibiotic strategies for the prevention of infectious complications following prostate biopsy: a systematic review and meta-analysis. J Urol. 2021;205(3):653–63.

39. Wegelin O, Exterkate L, van der Leest M, Kelder JC, Bosch JLHR, Barentsz JO, et al. Complications and adverse events of three magnetic resonance imaging-based target biopsy techniques in the diagnosis of prostate cancer among men with prior negative biopsies: results from the FUTURE trial, a multicentre randomised controlled trial. Eur Urol Oncol. 2019;2(6):617–24.

40. Hu JC, Assel M, Allaf ME, Ehdaie B, Vickers AJ, Cohen AJ, et al. Transperineal versus transrectal magnetic resonance imaging-targeted and systematic prostate biopsy to prevent infectious complications: the PREVENT randomized trial. Eur Urol. 2024;86(1):61–8.

41. Uleri A, Baboudjian M, Tedde A, Gallioli A, Long-Depaquit T, Palou J, et al. Is there an impact of transperineal versus transrectal magnetic resonance imaging-targeted biopsy in clinically significant prostate cancer detection rate? A systematic review and meta-analysis. Eur Urol Oncol. 2023;6(6):621–8.

42. Zattoni F, Fasulo V, Kasivisvanathan V, Kesch C, Marra G, Martini A, et al. Enhancing prostate cancer detection accuracy in magnetic resonance imaging-targeted prostate biopsy: optimizing the number of cores taken. Eur Urol Open Sci. 2024;66:16–25.

Publisher's Note